NX··Y Halogen Bonds.
Comparison with NH··Y H-bonds and CX··Y Halogen Bonds

Binod Nepal and Steve Scheiner*
Department of Chemistry and Biochemistry
Utah State University
Logan UT 84322-0300

Abstract

Quantum calculations examine how the NH··Y H-bond compares to the equivalent NX··Y halogen bond, as well as to comparable CH/CX donors. Succinimide and saccharin, and their corresponding halogen-substituted derivatives, are chosen as the prototype NH/NX donors, paired with a wide range of electron donor molecules. The NH··Y H-bond is weakened if the bridging H is replaced by Cl, and strengthened by I; a Br halogen bond is roughly comparable to a H-bond. The lone pairs of the partner molecule are stronger electron donors than are π-systems. Whereas Coulombic forces represent the largest fraction of the attractive force in the H-bonds, induction energy is magnified in the halogen bonds, surpassing electrostatics in several cases. Mutation of NH/NX to CH/CX weakens the binding energy to roughly half its original value, while also lengthening the intermolecular distances by 0.3 - 0.8 Å.

*email: steve.scheiner@usu.edu

keywords: NBO; SAPT; molecular electrostatic potential; NH bond stretch

INTRODUCTION

The realm of noncovalent interactions is large and diverse and continues to grow. The H-bond (HB) has perhaps attracted the most attention over the past decades [1, 2], due to its widespread occurrence in important chemical and biological processes. The definition of a HB has greatly expanded from its original inception involving F, O, and N atoms to a growing list [3, 4] of less electronegative atoms as well as π-systems that can serve as electron donors. Many of the intrinsic concepts of the HB have been found to occur as well in related noncovalent bonds [5] where the bridging H is replaced by tetrel, pnicogen, chalcogen, halogen, and even the nominally unreactive aerogen atoms, in the eponymously named bonds [6-16].

Of the latter sorts of interactions, the halogen bond (XB) has the longest history of inquiry and has been successfully exploited in a number of fields such as crystal engineering, drug development and delivery, catalysis, anion binding and sensing, among many others. Like the HB, the XB owes some of its attractive force to an electrostatic attraction between the bridging atom with a certain amount of positive charge and a negative region of the acceptor molecule. A second contribution arises from charge transfer into the AH/AX σ* antibonding orbital, which typically weakens and lengthens this covalent bond. Due in large measure to its very high electronegativity and low polarizability, the F atom is a reluctant participant in halogen bonding, but the Cl, Br, and I atoms engage in XBs which typically grow stronger as the halogen atom becomes larger.

While a great deal has been learned over the years about XBs, most of the systems examined are limited to situations where the bridging halogen is bound to a carbon [17-31] or other atom [16, 32-37]. There is a surprising paucity of information available for systems containing a N-X bond. Taking the parallel world of HBs as an example, there are certainly commonalities between CH and NH HBs, but there are also some significant differences as well. For example, the CH bond often shortens when it engages in a HB and its stretching frequency shifts to the blue, both opposite to what is observed for NH donors. NH HBs are systematically stronger than those with CH donors. It is therefore of some importance to consider the corresponding questions for halogen bonds, viz. how NX halogen bond donors might differ from their CH congeners.

There is a certain amount of information currently available, albeit not as robust as one would like, in the literature about NX halogen bonds [38-40]. Most of this data is structural in nature and derives from crystal studies, as recently summarized by Troff et al [41]. The N-X XB bond in halosuccinimides [42-44] shows up as a short intermolecular contact. Even shorter distances are observed when the XB acceptor is an anion [41], an amine or triazine [45, 46], or an imine [47]. Halosaccharins have also been observed to engage in XBs [48],

including with water and pyridine as halogen acceptor [49]. A very recent study [50] paired halosaccharins with a series of pyridine-N-oxides.

But what remains lacking is a thorough and comprehensive body of information that directly relates and compares NX with CX halogen bonds. Some of the most pressing questions at present begin with a comparison of the energetic and electronic structural features of NX halogen bonds. How does changing the identity of the X atom in the NX bond affect the strength of the interaction, and how do these noncovalent bonds compare with the analogous NH HBs? What is the sensitivity of the NX XB to the nature of the partner electron donor molecule; how do π-donors compare with lone-pair donors? What are the relative contributions to NX HBs of principal attractive components: electrostatic, induction, and dispersion energy? How does the formation of a NX XB affect the length of the internal covalent N-X bond?

The goal of the present work is to attempt to answer these questions via quantum chemical calculations. We take as a starting point systems where there is available a significant amount of experimental data to serve as a check on the validity of the calculations. The succinimide and saccharin systems fulfill this role, harkening back to their recent study [41-50]. As described below, a wide range of electron donor molecules is considered, including both lone pair and π-donors, and molecules of varying donor ability. Among this list is included both pyridine and pyridine N-oxide, again because of the availability of prior experimental data.

COMPUTATIONAL METHODS

Most of the calculations were carried out via the Gaussian-09 package.[51] The geometries were optimized at the MP2 level of theory in conjunction with the aug-cc-pVDZ[52] basis set; the aug-cc-pVDZ-PP [53] pseudopotential was used for the heavier atoms I and Br. The basis sets were taken externally from the EMSL library.[54] Only geometries with non-negative frequencies were taken into consideration to ensure each obtained geometry is in fact a true minimum. The binding energies were calculated as the differences between the energy of the complex and the sum of the monomers, corrected for basis set superposition error using the counterpoise procedure. Charge transfer was examined by Natural Bond Orbital (NBO)[55] calculations using the NBO 6.0 program.[56] The binding energies were decomposed into various components using Symmetry Adapted Perturbation Theory (SAPT)[57] via the MOLPRO-2010 software package.[58] The HF level of theory and the 6-31+G* basis set for lighter elements, and LANL2DZ basis sets for Br and I, was used for the SAPT analysis, as well as for the comparable MP2 interaction energy calculations. Extrapolation to complete basis set was performed via a method originally proposed by Truhlar[59] and which has been shown to work well for systems of this type[60]. ChemCraft software[61] was

used for visualization of geometries and vibrational frequencies. The molecular electrostatic potentials were analyzed by the Multiwfn software package.[62]

The molecular structures of succinimide and saccharin are displayed in Scheme I. The NH proton of each was replaced in turn by Cl, Br, and I so as to enable the formation of halogen bonds. The nine electron donors considered here are illustrated in Scheme I. They include those that donate electrons via lone pairs, as well as π-donors ethene, acetylene, and benzene.

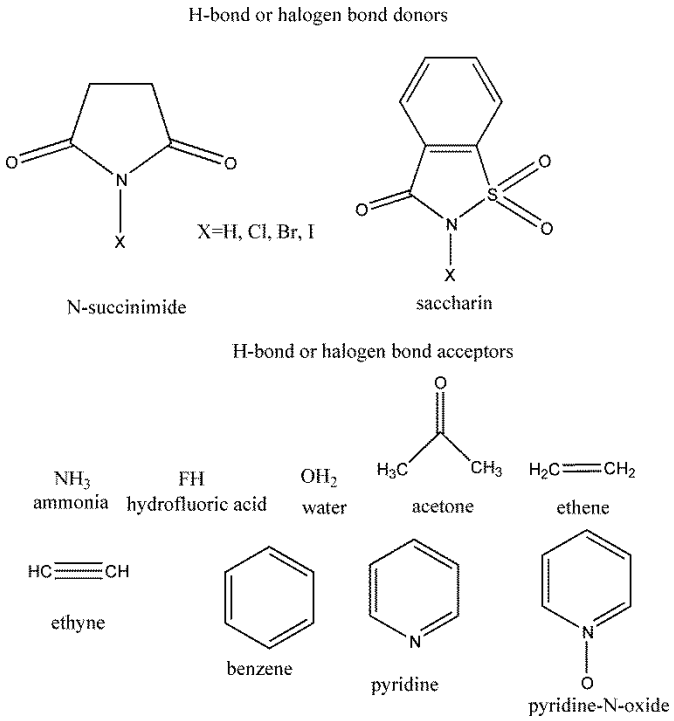

Scheme 1. Molecules participating in HB or XB interactions.

RESULTS AND DISCUSSION

Optimized Geometries and Binding Energies

The optimized geometries of the H-bonded succinimide complexes with NH_3, H_2O, acetone, pyridine, and pyridine N-oxide are presented on the left side of Fig 1. The right side illustrates the structures of the X-bonded complexes, as exemplified by X=Br; the structures for the Cl and I dimers are very similar. The analogous diagrams of the π-complexes with C_2H_4, HCCH, and benzene are displayed in Fig 2. There is more diversity in the HF complexes, all of which are illustrated in Fig 3. (The coordinates of all optimized geometries are listed in the Supporting Information.) Considering the structures in Fig 1, the X-bonded

geometries on the right side are all simple and straightforward XBs, with θ(NX··Y) ~ 180°. In contrast, the H-bonded geometries on the left all contain indications of a secondary HB, albeit a weak one in several cases. One of the H atoms of NH_3, for example, is oriented so as to form a secondary NH··O HB. The OH··O HB in the complex with water is as short as the "primary" NH··O HB. There is some geometrical evidence of subsidiary CH··O HBs in the other HB geometries in Fig 1. A secondary HB, also CH··O, appears likely in the HB geometry of acetylene in Fig 2. Turning to HF in Fig 3, its FH··O HB is shorter and likely stronger than the NH··F HB. When the H atom of succinimide is changed to Cl, this atom is not a strong enough halogen-bonder so one does not see a XB but rather a FH··O HB. Br and I, on the other hand, engage in strong enough XBs that one does see such F··X HBs.

The BSSE-corrected binding energies are reported in Table 1. Focusing first on the HB geometries in the first column, succinimide engages in fairly strong complexes when interacting with lone pairs, with binding energies in the 8-10 kcal/mol range. HBs with the π-systems are weaker, between 3.5 and 5.5 kcal/mol, in the order ethene < acetylene < benzene. (The binding energy of acetylene is likely inflated by the presence of the secondary CH··O HB, as is the case also for the OH··O HB for H_2O.) The XB structures in the next three columns obey a consistent pattern: Cl < Br < I. As a general rule of thumb, I XBs are roughly twice as strong as Cl XBs. In most cases, the HB binding energy falls between Br and I. These trends are true whether the bond is formed to lone pairs, or to π-systems. There is one distinction between HB and XB complexes. Ethene forms stronger XBs than does acetylene, in contrast to the HB pattern where it is acetylene that engages in stronger interactions. However, the HB energy of acetylene is likely inflated by the presence of the secondary CH··O HB. Whether HB or XB, pyridine and pyridine-N-oxide form substantially stronger complexes than do the other electron donors studied here.

Table 2 lists the intermolecular distances of the various optimized complexes. In most cases, the HBs are shorter than XBs, not surprising in view of the much smaller atomic radius for H. Within the class of XBs there are two competing trends. The increasing atomic radii would tend toward Cl < Br < I, but the strengthening bond that is associated with larger halogens would push toward an opposite pattern. The final result is a compromise wherein Br generally has the shortest XB and Cl the longest. There is an exception to this trend involving acetone wherein the Cl··O distance is shorter than that for Br, probably due to the presence of a CH··O HB in the former case which draws the two molecules together.

The lower halves of Tables 1 and 2 allow a comparison of succinimide with saccharin. The latter differs from the former first by the presence of a phenyl group fused to its five-membered ring. Also, one of the two CO groups adjacent to the NX group is replaced by a SO_2 unit. These replacements lead to an overall strengthening of the various bonds, both H and X. The increments are largest for the HBs, ranging

up to 2.4 kcal/mol, whereas the increases for the XBs are less than 1 kcal/mol. Importantly, the patterns are largely retained. I-bonds are the strongest of the halogen bonds, and Cl-bonds the weakest. HBs are usually a bit weaker than I-bonds but there are a few exceptions where the reverse if observed, e.g. acetone, pyridine-N-oxide, acetylene, and benzene. The former can be explained by the presence of a pair of CH··O HBs that add to the stability of the HB configuration, while the others would appear to be an intrinsic property of the systems involved.

As a last bit of geometrical information, it is well known that the formation of a HB or XB will typically elongate the pertinent N-H or N-X covalent bond. These bond stretches are contained in Table 3 and reproduce some of the energetic trends in Table 1 but not all. Like the binding energies, the stretches increase in the order Cl < Br < I. On the other hand, the NH stretch is less than that for X=Br, although the HB energy is greater than the Br-bond energy. Within the subset of π-donors, the energetic order acetylene < ethene < benzene is altered, with ethene showing the largest bond stretch and acetylene the smallest. The uniformly stronger bonds formed by saccharin vs succinimide are less consistent with respect to bond stretches.

There is always the question as to how well any particular level of theory reproduces data that might be computed at a higher level. In order to address this issue, succinimide, and its three variants of halosubstituted derivatives, was paired with both NH_3 and OH_2, and the binding energies computed at higher levels. The results, displayed in Table 4, show that enlargement of basis set from aug-cc-pVDZ to aug-cc-pVTZ, and then extrapolated to complete basis set, each result in a small increase in binding energy, but less than 1 kcal/mol. On the other hand, the improvement of the treatment of electron correlation from MP2 to CCSD(T) leads to only a very small decrease, suggesting MP2 is quite good for treatment of these systems. As a final point of comparison, the M06-2X variant of DFT uniformly overestimates the binding energies, whether compared with MP2 or with CCSD(T).

Electronic Structure Analysis

A myriad of prior studies have pointed to electrostatic attraction as a primary component of both H and X bonds. For that reason, it is instructive to inspect the molecular electrostatic potential (MEP) that surrounds each of the proton or halogen-donor molecules being considered here. These potentials are displayed in Fig 4 wherein blue and red regions correspond respectively to positive and negative regions of the MEP. Each of the molecules contains a blue area at the site of its bonding, i.e. its H or X atom. This blue area is smallest for X=Cl and grows larger for Br and I, and is even broader for H. The numerical values in Fig 4 refer to the value of the potential where it reaches its maximal value, $V_{s,max}$, on the contour wherein the electron density is fixed at 0.001 au. These quantities increase in the same Cl < Br < I < H

order as the size of the blue region. There are only small differences between the succinimide values in the top of Fig 4 and the saccharin quantities in the lower half. It is perhaps important to note that even though X=H is associated with the largest $V_{s,max}$ values, the binding energies of the HB complexes are usually surpassed by those for X=I.

While the MEPs provide useful insights into the electrostatic interactions, they are silent concerning the effects of mutual polarization and charge transfer between the two subunits in each complex. The latter can be understood via NBO analysis which quantifies the energetic consequences of charge transfer between pairs of individual orbitals. It is known that the largest share of charge in H or X-bonded systems is transferred into the σ*(NX) antibonding orbital. These quantities are displayed in Table 5 where the donating orbital is either the lone pair(s) or the π-orbitals of the electron donor molecule. It must be recalled that in those cases where a secondary interaction occurs, there are other important charge transfers. For example, the 9.61 kcal/mol E(2) for the HB complex of succinimide with OH_2 is supplemented by an additional 9.08 kcal/mol by the transfer into the σ*(OH) antibonding orbital of the water from the OH··O HB.

With the obvious exception of those cases of a strong secondary interaction, the E(2) quantities mirror the binding energies in Table 1 fairly well. Taking the HB systems with succinimide as an example, the acetone < NH_3 < pyridine < pyridine-N-oxide trend in binding energy is the same order as is observed for E(2). The two quantities are even more closely related for the set of six I-bonding systems: FH < OH_2 < acetone < NH_3 < pyridine-N-oxide < pyridine. There are also parallels in that both E(2) and binding energy follow the general pattern of Cl < Br < H < I. The quantities are not as closely related for the various π-complexes in that E(2) is largest for ethene but benzene is more strongly bound. Part of this discrepancy may be related to a secondary charge transfer from the halogen lone pair to the π* orbitals of the alkene.

Given the large values of some of the NBO quantities in Table 5, it was considered prudent to examine how sensitive they might be to basis set[63]. Parallel calculations were thus carried out for the aug-cc-pVTZ basis set, and the data compared with aug-cc-pVDZ. Examination focused on those systems with the largest values of E(2) to check for possible basis set inflation. A reduction was observed with the larger basis set, but this decrease was fairly small, only 4-12%, for the I-bonded structures that show the largest values of E(2). For example, E(2) was reduced from 42.2 kcal/mol for the succinimide-I complex with pyridine-N-oxide to 38.7 kcal/mol with the larger basis.

The decomposition of the total binding energy into separate components, each with a physical significance, can add further insights into the nature of the bonding. The various SAPT components of the interactions are listed in Tables S1 and S2. In order to place these quantities into an instructive perspective,

it is useful to display them graphically. Fig 5 illustrates the fractional contribution of each of the electrostatic (ES, blue), induction (IND, red) and dispersion (DISP, green) components to their total, the entire attractive energy in the complexes containing succinimide. The distinction between H and X bonds is immediately apparent. The blue electrostatic energy accounts for a large share of the total attraction for the H-bonds in Fig 5a, more than 50% in most cases. Induction makes a smaller contribution 20-30%, followed by dispersion at less than 20%. The principal exception is the H-bond to benzene, where the three components are roughly equal. This disproportionately large ES contribution is consistent with the larger values of $V_{s,max}$ for the H-bonding molecules in Fig 4.

The pattern is different for the halogen bonds in Fig 5. In the first place, induction energy is comparable to and sometimes larger than the electrostatic component. The larger induction is especially noticeable for the three π-systems on the right side, where IND hovers around 50%. But even for the XBs formed to the lone pairs on the left, IND is nearly as large as ES. Where the HBs and XBs are most similar is in the percentage contribution of DISP, which is the smallest of the three components. As may be seen in Fig S1, the three components compose very similar percentages of the total attraction for the corresponding saccharin complexes.

The absolute magnitudes of the various quantities also offer insights into the nature of the interactions. With regard to each attractive term, one sees a clear Cl < Br < I trend. This pattern is especially noticeable with respect to induction energy, where it can increase by a factor of as much as 4 between Cl and I. While obeying the same pattern, dispersion is not quite as sensitive to the nature of the halogen atom. With respect to the nature of the electron donor species, pyridine and pyridine-N-oxide exhibit the largest components in general. Induction and dispersion are disproportionately large for the π-donors ethene, acetylene, and benzene. The latter is associated with especially high dispersion, while the former shows large induction. The quantities related to H are a bit more variable but generally hover between Cl and I.

In order to assess the degree of correlation between interaction energies computed via SAPT analysis, with that arising from a counterpoise correction of the MP2 treatment with the same basis set, the latter are displayed in the final column of Tables S1 and S2. (Note that the latter values, as well as SAPT quantities, refer to interaction energies, rather than the binding energies discussed above.) In most cases, MP2 and SAPT yield quite similar interaction energies. Indeed, the correlation for linear fitting of the two amounts to 0.95.

DISCUSSION

The generally lesser ability of π-systems, as compared to lone pairs, to donate protons to XBs matches earlier findings for related pnicogen and chalcogen bonds [64-67]. The Cl < Br < H < I order of binding

energy of the N-X donors examined here is consistent with similar patterns observed previously for the many C-X donors that have been studied in the past [25, 68-75].

It is already well established that NH H-bonds are typically considerably stronger than the related CH HBs. But the comparisons between NX and CX halogen bonds remain relatively unexplored. This issue was examined here in a direct manner by replacing the NH of succinimide by CH_2, so as to retain the basic structure and internal bonding. The resulting 1,3-cyclopentadione was thus taken as the CH donor, and XBs were formed by replacing one of the two H atoms by F, Cl, Br, and I in turn. Each of these molecules was then paired with NH_3 as prototypical electron donor. The counterpoise-corrected binding energies are presented in Table 6, along with the optimized intermolecular distances. Also contained in Table 6 are the corresponding data for the analogous NH/NX donor succinimide. (Like the complex with succinimide, the H-bonding cyclopentadione complex with NH_3 also contains secondary attractive interactions in addition to the HB.) The first row of Table 6 confirms the weaker CH··N HB, as compared to NH··N by a factor of ½. In fact, this weakening CX/NX ratio is fairly typical of the XBs as well. Consistent with their weaker nature, the various CH/CX complexes are also characterized by longer intermolecular separations, by 0.3 Å for the three XBs, and by 0.8 Å for the HBs.

Another comparison between N and C H/X donors derives from a prior M06-2X/aug-cc-pVDZ study of the CI··N bond between pentafluoroiodobenzene and pyridine[76] which obtained a binding energy of 6.9 kcal/mol. This quantity is considerably smaller than the 12.8 kcal/mol calculated here for the NI··N bond between I-succinimide and pyridine. Pentafluoroiodobenzene was also the I-donor with acetone in another study.[77] At the same level of theory used here, this CI··O XB had a binding energy of 4.9 kcal/mol, less than the 7.6 and 8.5 kcal/mol respectively calculated above for the NI··O bond between acetone and both I-succinimide and I-saccharin. Moreover, this quantity dropped further when some of the electron-withdrawing F atoms were removed from the I donor of the CI··O bond.

A very recent set of calculations [74] dealing with simpler systems affirmed the weaker CX XBs in a set of methyl halide oligomers when compared to the analogous NX XBs in aminohalides, wherein the former amount to roughly 60% of the latter. This weakening is not very different than the 50% reduction noted above for our comparison of succinimide with cyclopentadione in Table 5. Calculations on the nitrohalides [78, 79] affirmed the I > Br > Cl trend of NX HBs. Recent work by McDowell and Maynard [80] computed the cooperativity experienced by a N-Cl XB when the N atom acts simultaneously as electron donor, but did not draw parallels with the analogous C-Cl XB. With regard to the energy decomposition, earlier calculations [81-83] had also concluded that both dispersion and charge transfer were vital ingredients in XBs, in addition to electrostatics.

There are experimental results available with which we can directly compare some of our data. Puttreddy et al [50] reported the solid state geometrical parameters for complexes of I-succinimide and I-saccharin with pyridine-N-oxide, and Makhotina et al [48] reported analogous quantities for pyridine. In Table 7, the numbers outside and inside the parentheses respectively represent our calculated parameters and experimental values from the crystal. The internal N-I bond lengths are reproduced very well by the calculations, while the calculated XB R(I···O/N) distances are a bit longer (by about 0.1 Å). The intermolecular distances in the crystal may be shortened by the strengthening effects of cooperative interactions with neighboring molecules. The XB angles in the final column of Table 7 are all close to linearity, both experimental and computed. The association constants measured by Puttreddy et al [50] were also consistent with our finding (Table 1) that pyridine-N-oxide is considerably more strongly bound with I-succinimide than are water or acetone. The results of Makhotina et al [48] offer additional support for our calculated finding that I-saccharin forms a stronger I-bond with pyridine than does I-succinimide.

In summary, the calculations presented here indicate that the strength of a XB with Cl as donor is much weaker than the corresponding HB. Replacement of Cl by Br yields a XB that is of comparable strength to the corresponding HB, while I presents the strongest interaction of all. Lone pair electron donors lead to stronger interactions than π-donors, particularly pyridine and pyridine-N-oxide. Mutation of succinimide to the larger NX donor saccharin results in a modest enhancement of the binding. The strengths of the interactions correspond to the NBO charge transfer energies E(2) and to the intensity of the positive MEP in the vicinity of the binding atom, whether H or X, although these correlations are imperfect. Decomposition of the binding energies suggests that electrostatics account for the lion's share of the HB. The induction energy is substantially larger for the XBs, surpassing electrostatics in a number of cases.

ACKNOWLEDGMENTS

Computer, storage and other resources from the Division of Research Computing in the Office of Research and Graduate Studies at Utah State University are gratefully acknowledged.

SUPPORTING INFORMATION

SAPT components of complexes, along with Cartesian coordinates of optimized geometries.

REFERENCES

1. G. Gilli and P. Gilli, *The Nature of the Hydrogen Bond*, Oxford University Press, Oxford, UK, 2009.
2. S. Scheiner, *Hydrogen Bonding. A Theoretical Perspective*, Oxford University Press, New York, 1997.
3. S. J. Grabowski, ed. *Hydrogen Bonding - New Insights*, Springer, Dordrecht, Netherlands, 2006.
4. E. Arunan, G. R. Desiraju, R. A. Klein, J. Sadlej, S. Scheiner, I. Alkorta, D. C. Clary, R. H. Crabtree, J. J. Dannenberg, P. Hobza, H. G. Kjaergaard, A. C. Legon, B. Mennucci and D. J. Nesbitt, *Pure Appl. Chem.*, 2011, **83**, 1637-1641.
5. S. Scheiner, ed. *Noncovalent Forces*, Springer, Heidelberg, 2015.
6. A. Bauzá and A. Frontera, *Angew. Chem. Int. Ed.*, 2015, **54**, 7340-7343.
7. M. D. Esrafili and F. Mohammadian-Sabet, *Mol. Phys.*, 2016, **114**, 1528-1538.
8. S. J. Grabowski, *Phys. Chem. Chem. Phys.*, 2014, **16**, 1824-1834.
9. S. Scheiner, *J. Phys. Chem. A*, 2015, **119**, 9189-9199.
10. C. Bleiholder, D. B. Werz, H. Koppel and R. Gleiter, *J. Am. Chem. Soc.*, 2006, **128**, 2666-2674.
11. R. Gleiter, D. B. Werz and B. J. Rausch, *Chem. Eur. J.*, 2006, **9**, 2676-2683.
12. P. Sanz, O. Mó and M. Yáñez, *Phys. Chem. Chem. Phys.*, 2003, **5**, 2942-2947.
13. U. Adhikari and S. Scheiner, *Chem. Phys. Lett.*, 2012, **532**, 31-35.
14. P. Metrangolo and G. Resnati, *Science*, 2008, **321**, 918-919.
15. T. Clark, M. Hennemann, J. S. Murray and P. Politzer, *J. Mol. Model.*, 2007, **13**, 291-296.
16. I. Alkorta, F. Blanco, M. Solimannejad and J. Elguero, *J. Phys. Chem. A*, 2008, **112**, 10856-10863.
17. J. P. M. Lommerse, A. J. Stone, R. Taylor and F. H. Allen, *J. Am. Chem. Soc.*, 1996, **118**, 3108-3116.
18. P. L. Wash, S. Ma, U. Obst and J. Rebek, *J. Am. Chem. Soc.*, 1999, **121**, 7973-7974.
19. P. Auffinger, F. A. Hays, E. Westhof and P. S. Ho, *Proc. Nat. Acad. Sci., USA*, 2004, **101**, 16789-16794.
20. P. Metrangolo, H. Neukirch, T. Pilati and G. Resnati, *Acc. Chem. Res.*, 2005, **38**, 386-395.
21. P. Politzer, P. Lane, M. C. Concha, Y. Ma and J. S. Murray, *J. Mol. Model.*, 2007, **13**, 305-311.
22. V. d. P. N. Nziko and S. Scheiner, *Phys. Chem. Chem. Phys.*, 2016, **18**, 3581-3590.
23. K. Raatikainen and K. Rissanen, *Cryst. Growth Des.*, 2010, **10**, 3638-3646.
24. M. D. Esrafili and N. L. Hadipour, *Mol. Phys.*, 2011, **109**, 2451-2460.
25. B. Nepal and S. Scheiner, *Chem. Eur. J.*, 2015, **21**, 13330-13335.
26. S. J. Grabowski, *J. Phys. Chem. A*, 2011, **115**, 12340-12347.
27. A. Bauzá, D. Quiñonero, A. Frontera and P. M. Deyà, *Phys. Chem. Chem. Phys.*, 2011, **13**, 20371-20379.
28. I. Alkorta, G. Sanchez-Sanz and J. Elguero, *CrystEngComm*, 2013, **15**, 3178-3186.
29. D. Hauchecorne and W. A. Herrebout, *J. Phys. Chem. A*, 2013, **117**, 11548-11557.
30. K. E. Riley, C. L. Ford Jr and K. Demouchet, *Chem. Phys. Lett.*, 2015, **621**, 165-170.
31. V. d. P. N. Nziko and S. Scheiner, *J. Org. Chem.*, 2016, **81**, 2589-2597.
32. I. Alkorta, S. Rozas and J. Elguero, *J. Phys. Chem. A*, 1998, **102**, 9278-9285.
33. A. Karpfen, in *Halogen Bonding. Fundamentals and Applications*, eds. P. Metrangolo and G. Resnati, Springer, Berlin2008, vol. 126, pp. 1-15.
34. P. Politzer, J. S. Murray and M. Concha, *J. Mol. Model.*, 2008, **14**, 659-665.
35. S. Scheiner, *Int. J. Quantum Chem*, 2013, **113**, 1609-1620.
36. Q. Li, X. Xu, T. Liu, B. Jing, W. Li, J. Cheng, B. Gong and J. Sun, *Phys. Chem. Chem. Phys.*, 2010, **12**, 6837-6843.
37. A. C. Legon, *Phys. Chem. Chem. Phys.*, 2010, **12**, 7736-7747.

38. M. Bedin, A. Karim, M. Reitti, A.-C. C. Carlsson, F. Topic, M. Cetina, F. Pan, V. Havel, F. Al-Ameri, V. Sindelar, K. Rissanen, J. Grafenstein and M. Erdelyi, *Chem. Sci.*, 2015, **6**, 3746-3756.
39. S. B. Hakkert and M. Erdélyi, *J. Phys. Org. Chem.*, 2015, **28**, 226-233.
40. P. V. Gushchin, M. L. Kuznetsov, M. Haukka and V. Y. Kukushkin, *J. Phys. Chem. A*, 2013, **117**, 2827-2834.
41. R. W. Troff, T. Mäkelä, F. Topić, A. Valkonen, K. Raatikainen and K. Rissanen, *Eur. J. Org. Chem.*, 2013, **2013**, 1617-1637.
42. R. Brown, *Acta Cryst.*, 1961, **14**, 711-715.
43. O. Jaray, H. Pritzow and J. Jander, *Z. Naturforsch B*, 1977, **32**, 1416-1420.
44. K. Padmanabhan, I. C. Paul and D. Y. Curtin, *Acta Crystallographica Section C*, 1990, **46**, 88-92.
45. K. Raatikainen and K. Rissanen, *CrystEngComm*, 2011, **13**, 6972-6977.
46. E. H. Crowston, A. M. Lobo, S. Parbhakar, H. S. Rzepa and D. J. Williams, *J. Chem. Soc., Chem. Commun.*, 1984, 276-278.
47. I. Castellote, M. Moron, C. Burgos, J. Alvarez-Builla, A. Martin, P. Gomez-Sal and J. J. Vaquero, *Chem. Commun.*, 2007, 1281-1283.
48. O. Makhotkina, J. Lieffrig, O. Jeannin, M. Fourmigué, E. Aubert and E. Espinosa, *Cryst. Growth Des.*, 2015, **15**, 3464-3473.
49. D. Dolenc and B. Modec, *New J. Chem.*, 2009, **33**, 2344-2349.
50. R. Puttreddy, O. Jurcek, S. Bhowmik, T. Makela and K. Rissanen, *Chem. Commun.*, 2016, **52**, 2338-2341.
51. M. J. Frisch, G. W. Trucks, H. B. Schlegel, G. E. Scuseria, M. A. Robb, J. R. Cheeseman, G. Scalmani, V. Barone, B. Mennucci, G. A. Petersson, H. Nakatsuji, M. Caricato, X. Li, H. P. Hratchian, A. F. Izmaylov, J. Bloino, G. Zheng, J. L. Sonnenberg, M. Hada, M. Ehara, K. Toyota, R. Fukuda, J. Hasegawa, M. Ishida, T. Nakajima, Y. Honda, O. Kitao, H. Nakai, T. Vreven, J. A. Montgomery Jr., J. E. Peralta, F. Ogliaro, M. J. Bearpark, J. Heyd, E. N. Brothers, K. N. Kudin, V. N. Staroverov, R. Kobayashi, J. Normand, K. Raghavachari, A. P. Rendell, J. C. Burant, S. S. Iyengar, J. Tomasi, M. Cossi, N. Rega, N. J. Millam, M. Klene, J. E. Knox, J. B. Cross, V. Bakken, C. Adamo, J. Jaramillo, R. Gomperts, R. E. Stratmann, O. Yazyev, A. J. Austin, R. Cammi, C. Pomelli, J. W. Ochterski, R. L. Martin, K. Morokuma, V. G. Zakrzewski, G. A. Voth, P. Salvador, J. J. Dannenberg, S. Dapprich, A. D. Daniels, Ö. Farkas, J. B. Foresman, J. V. Ortiz, J. Cioslowski and D. J. Fox, Gaussian, Inc., Wallingford, CT, USA2009.
52. D. E. Woon and T. H. Dunning, *J. Chem. Phys.*, 1993, **98**, 1358-1371.
53. K. A. Peterson, B. C. Shepler, D. Figgen and H. Stoll, *J. Phys. Chem. A*, 2006, **110**, 13877-13883.
54. K. L. Schuchardt, B. T. Didier, T. Elsethagen, L. Sun, V. Gurumoorthi, J. Chase, J. Li and T. L. Windus, *J. Chem. Inf. Model.*, 2007, **47**, 1045-1052.
55. J. P. Foster and F. Weinhold, *J. Am. Chem. Soc.*, 1980, **102**, 7211-7218.
56. E. D. Glendening, C. R. Landis and F. Weinhold, *J. Comput. Chem.*, 2013, **34**, 1429-1437.
57. K. Szalewicz, *WIREs Comput Mol Sci*, 2012, **2**, 254-272.
58. H.-J. Werner, P. J. Knowles, G. Knizia, F. R. Manby and M. Schütz, *WIREs Comput Mol Sci*, 2012, **2**, 242-253.
59. D. G. Truhlar, *Chem. Phys. Lett.*, 1998, **294**, 45-48.
60. S. Scheiner, *Comp. Theor. Chem.*, 2012, **998**, 9-13.
61. G. A. Andrienko, *http://www.chemcraftprog.com*.
62. T. Lu and F. Chen, *J. Comput. Chem.*, 2012, **33**, 580-592.
63. K. U. Lao and J. M. Herbert, *J. Chem. Theory Comput.*, http://dx.doi.org/10.1021/acs.jctc.6b00155
64. S. Scheiner and U. Adhikari, *J. Phys. Chem. A*, 2011, **115**, 11101-11110.
65. M. D. Esrafili and F. Mohammadian-Sabet, *Mol. Phys.*, 2015, **113**, 3559-3566.
66. A. Bauzá and A. Frontera, *ChemPhysChem*, 2015, **16**, 3108-3113.

67. F. Zhou, R. Liu, P. Li and H. Zhang, *New J. Chem.*, 2015, **39**, 1611-1618.
68. S. W. L. Hogan and T. van Mourik, *J. Comput. Chem.*, 2016, **37**, 763-770.
69. M. D. Esrafili and M. Vakili, *Mol. Phys.*, 2016, **114**, 325-332.
70. S. A. C. McDowell and Z. L. Holder, *Mol. Phys.*, 2015, **113**, 3757-3766.
71. Y.-Z. Zheng, G. Deng, Y. Zhou, H.-Y. Sun and Z.-W. Yu, *ChemPhysChem*, 2015, **16**, 2594-2601.
72. B. Nepal and S. Scheiner, *J. Phys. Chem. A*, 2015, **119**, 13064-13073.
73. Y. Geboes, N. Nagels, B. Pinter, F. De Proft and W. A. Herrebout, *J. Phys. Chem. A*, 2015, **119**, 2502-2516.
74. J. Dominikowska, F. M. Bickelhaupt, M. Palusiak and C. Fonseca Guerra, *ChemPhysChem*, 2016, **17**, 474-480.
75. B. Nepal and S. Scheiner, *ChemPhysChem*, 2016, **17**, 836-844.
76. Q. Shi, H. Su, Y. Liu, W. Wu and Y. Lu, *Comp. Theor. Chem.*, 2014, **1027**, 79-83.
77. K. E. Riley, J. S. Murray, J. Fanfrlík, J. Řezáč, R. J. Solá, M. C. Concha, F. M. Ramos and P. Politzer, *J. Mol. Model.*, 2011, **17**, 3309-3318.
78. M. Solimannejad, V. Ramezani, C. Trujillo, I. Alkorta, G. Sánchez-Sanz and J. Elguero, *J. Phys. Chem. A*, 2012, **116**, 5199-5206.
79. M. Solimannejad, N. Nassirinia and S. Amani, *Struct. Chem.*, 2013, **24**, 651-659.
80. S. A. C. McDowell and S. J. Maynard, *Mol. Phys.*, 2016, **114**, 1609-1618.
81. M. Carter, A. K. Rappé and P. S. Ho, *J. Chem. Theory Comput.*, 2012, **8**, 2461-2473.
82. P. Deepa, B. V. Pandiyan, P. Kolandaivel and P. Hobza, *Phys. Chem. Chem. Phys.*, 2014, **16**, 2038-2047.
83. J. Thirman and M. Head-Gordon, *J. Chem. Phys.*, 2015, **143**, 084124.

Table 1. Counterpoise-corrected binding energies (kcal/mol) of H and X bonded complexes

Succinimide systems				
	H	Cl	Br	I
NH_3	8.20	3.83	7.09	9.83
OH_2	8.22[d]	2.52	4.11	5.43
FH	10.09[a]	7.22[b]	2.00	2.48
acetone	7.60	3.81	5.83	7.58
pyridine	10.04	5.12	9.21	12.77
Pyridine-N-oxide	10.33	5.63	8.23	10.95
π-complexes				
ethene	3.46	2.37	3.93	5.15
acetylene	4.38	2.16	3.24	4.05
benzene	5.46[c]	3.14	4.46	5.56
Saccharin complexes				
	H	Cl	Br	I
NH_3	9.65	4.12	7.91	11.28
OH_2	7.92 [d]	2.60	4.33	5.92
FH	9.57 [a]	5.51[b]	2.07	2.69
acetone	8.77[e]	3.96	6.14	8.48
pyridine	11.53	5.43	10.39	14.66
Pyridine-N-oxide	12.76	6.22	8.79	12.52
π-complexes				
ethene	4.38	2.59	4.36	5.90
acetylene	4.58	2.18	3.37	4.40
benzene	7.29	3.86	4.75	6.15

[a]FH acts as the proton acceptor from NH and as donor to O

[b]no halogen bond; FH acts as the proton donor to O

[c]small negative frequency

[d]NH··O supplemented by OH··O

[e]stabilized by pair of CH··O HBs

Table 2. Intermolecular H/X bond distances (Å) of the optimized geometries.

Succinimide systems				
	H	Cl	Br	I
NH_3	1.935	2.754	2.608	2.653
OH_2	1.996	2.801	2.747	2.810
FH	2.154	-	2.421	3.000
acetone	1.853	2.739	2.907	2.677
pyridine	1.813	2.617	2.421	2.497
Pyridine-N-oxide	1.764	2.720	2.515	2.537
π-complexes				
ethene	2.375	3.046	2.633	2.968
acetylene	2.403	3.101	3.025	3.126
benzene	2.052	3.050	2.965	3.051
Saccharin complexes				
	H	Cl	Br	I
NH3	1.832	2.702	2.536	2.586
OH2	1.931	2.785	2.716	2.762
FH	2.100	-	2.869	2.969
acetone	1.842	2.710	2.588	2.618
pyridine	1.713	2.579	2.332	2.434
Pyridine-N-oxide	1.656	2.723	2.451	2.472
π-complexes				
ethene	2.384	2.997	2.838	2.881
acetylene	2.302	3.070	2.980	3.060
benzene	2.164	3.166	2.968	2.997

Table 3. Stretch (mÅ) of the covalent bond, Δr(N-H/X) caused by the formation of the HB/XB.

Succinimide systems				
	H	Cl	Br	I
NH_3	19.2	13.4	32.9	44.7
OH_2	7.9	4.2	8.9	13.6
FH	4.89	-	1.86	3.19
acetone	14.7	5.4	14.9	22.8
pyridine	28.5	19.2	56.1	66.2
Pyridine-N-oxide	23.1	7.8	27.2	41.3
π-complexes				
ethene	4.5	7.3	19.0	26.1
acetylene	4.3	4.2	9.9	12.9
benzene	2.7	3.5	12.0	16.8
Saccharin complexes				
	H	Cl	Br	I
NH3	29.8	13.8	37.5	43.5
OH2	10.8	2.4	6.2	4.4
FH	2.9	-	0.1	-5.7
acetone	14.8	7.4	12.9	17.5
pyridine	43.4	21.4	73.6	71.5
Pyridine-N-oxide	41.0	6.4	30.8	41.2
π-complexes				
ethene	3.7	8.6	22.6	24.2
acetylene	5.7	4.6	9.8	5.7
benzene	4.0	-0.3	12.2	11.3

Table 4. Comparisons of counterpoise-corrected binding energies (kcal/mol) with different methods for H and X-bonded complexes for succinimide systems.

	MP2 aug-cc-pVDZ	MP2 aug-cc-pVTZ	MP2 CBS	CCSD(T) aug-cc-pVDZ	M06-2X aug-cc-pVDZ
H···NH_3	8.20	8.76	9.19	7.97	8.85
H···OH_2	8.22	8.84	9.30	8.19	9.55
Cl···NH_3	3.83	4.14	4.42	3.65	4.34
Cl···OH_2	2.52	2.70	2.87	2.47	3.03
Br···NH_3	7.09	7.34	7.68	6.90	7.94
Br···OH_2	4.11	4.25	4.47	4.01	5.12
I···NH_3	9.83	9.99	10.36	9.24	11.29
I···OH_2	5.43	5.56	5.81	5.28	7.07

Table 5. NBO charge transfer energies E(2) for transfer into σ*(NH/X) antibonding orbital. All in kcal/mol.

Succinimide systems				
	H	Cl	Br	I
NH_3	23.99	8.17	23.05	34.58
OH_2	9.61	3.86	8.38	13.13
FH	4.03	-	3.27	4.91
acetone	21.83	4.57	13.21	21.68
pyridine	31.23	10.78	37.36	49.81
Pyridine-N-oxide	34.43	5.68	24.39	42.15
π-complexes				
ethene	7.24	4.34	12.17	19.63
acetylene	5.63	2.91	6.91	9.99
benzene	6.99	2.46	8.44	13.02
Saccharin complexes				
	H	Cl	Br	I
NH_3	36.11	9.87	29.82	43.36
OH_2	14.40	4.13	9.97	15.43
FH	5.12	-	3.85	5.41
acetone	20.88	5.21	15.76	26.81
pyridine	48.26	11.98	52.86	62.74
Pyridine-N-oxide	54.16	5.32	31.84	53.33
π-complexes				
ethene	7.05	5.19	15.48	26.19
acetylene	7.89	3.28	8.29	12.77
benzene	8.79	1.23	9.32	15.75

Table 6. Comparison of counterpoise-corrected binding energies and intermolecular distances for the complexes of substituted 1,3-cyclopentadione and succinimide with NH_3.

	E_b, kcal/mol		R(X··N), Å	
	1,3-cyclopentadione	succinimide	1,3-cyclopentadione	succinimide
H	4.31[a]	8.20	2.720	1.935
Cl	1.64	3.83	3.076	2.754
Br	4.91	7.09	2.944	2.608
I	5.42	9.83	2.945	2.653

[a] Not completely H-bonded complex

Table 7. Comparison of calculated with experimentally determined geometrical parameters, in parentheses.

complex	R(N-I), Å	R(I···O/N), Å	θ(N-I···O), degs
Succinimide-I···Pyridine-N-Oxide	2.090(2.094)	2.537(2.453)	173.(179)
Saccharin-I···Pyridine-N-Oxide	2.107(2.139)	2.472(2.328)	174(177)
Succinimide-I···Pyridine	2.115(2.116)	2.497(2.493)	180(180)
Saccharin-I···Pyridine	2.137(2.254)	2.434(2.254[a])	180(180)

[a] X-ray quality was reported to be poor

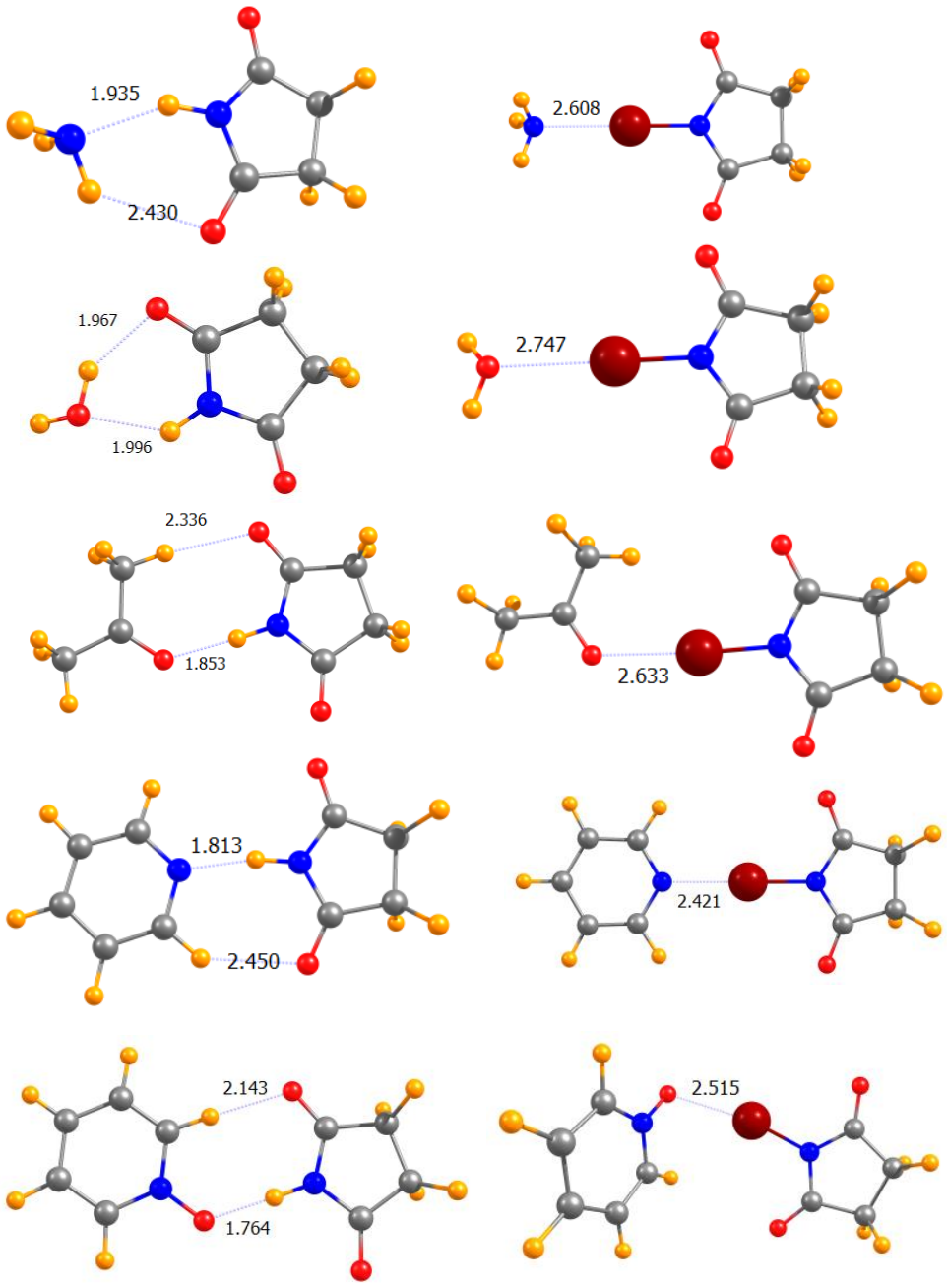

Fig 1. Geometries of complexes of succinimide and Br-succinimide with five lone-pair electron donors. Distances in Å.

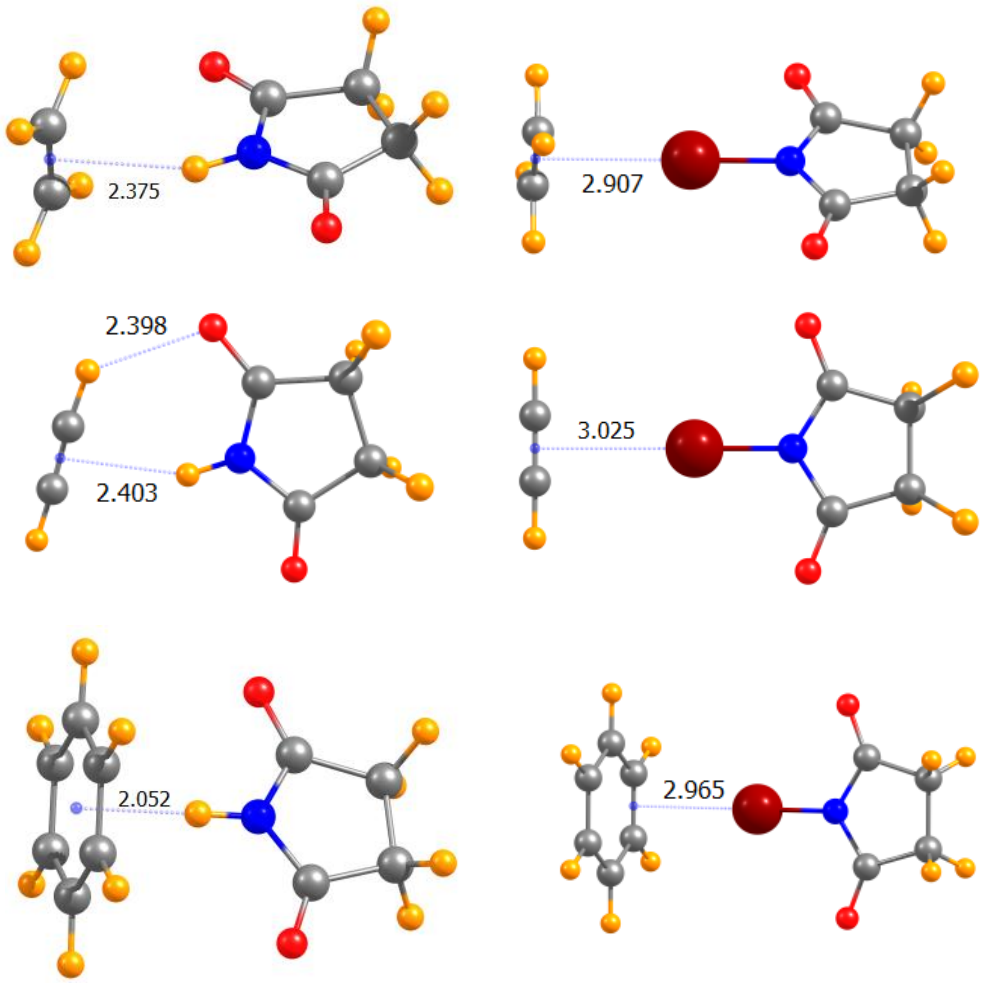

Fig 2. Geometries of complexes of succinimide and Br-succinimide with three π-electron donors. Distances in Å.

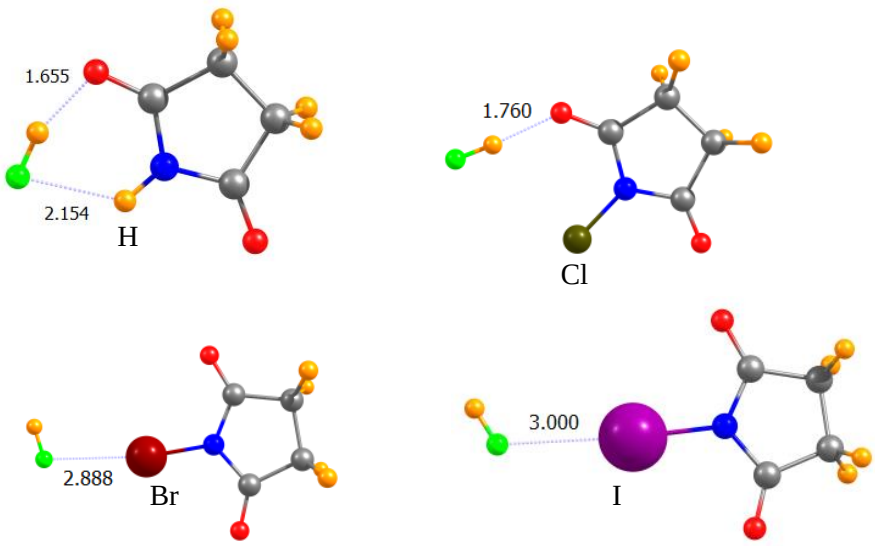

Fig 3. Geometries of complexes of HF with succinimide and halosuccinimides. Distances in Å.

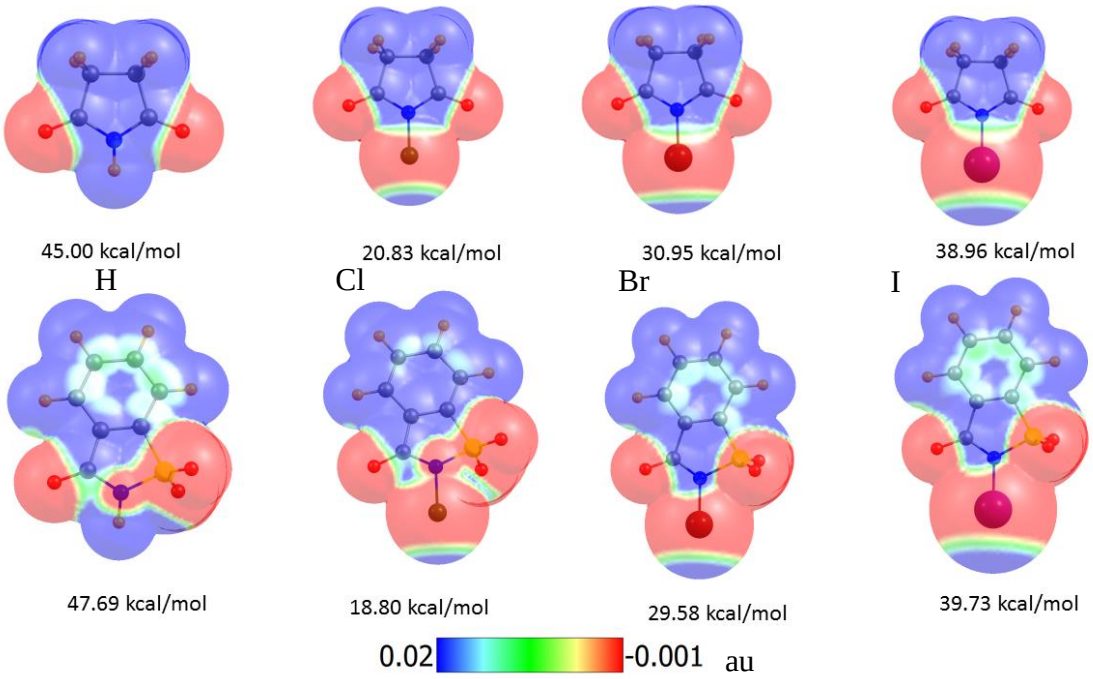

Fig 4. Molecular electrostatic potentials (MEPs) of succinimide (top) and saccharin (bottom), and their halosubstituted derivatives. Numerical values correspond to $V_{s,max}$.

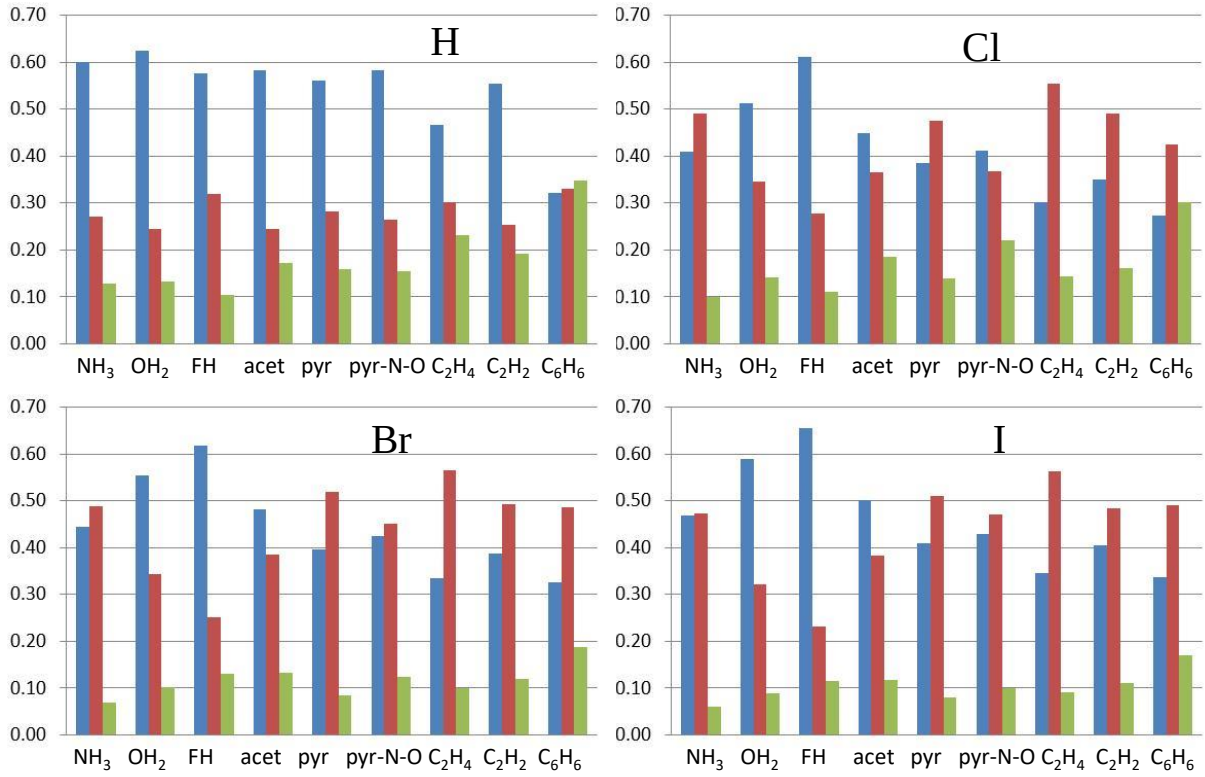

Fig 5. Fractional contributions of electrostatic (blue), induction (red), and dispersion (green) to total attraction energy in complexes with succinimide and its indicated halosubstituted derivatives.